Applied Physics Letters

Light extraction employing optical tunneling in blue InP quantum dot light-emitting diodes

Cite as: Appl. Phys. Lett. **120**, 091101 (2022); https://doi.org/10.1063/5.0084416
Submitted: 06 January 2022 • Accepted: 14 February 2022 • Published Online: 28 February 2022

Guanding Mei, Yangzhi Tan, Jiayun Sun, et al.

Applied Physics Letters ARTICLE scitation.org/journal/apl

Light extraction employing optical tunneling in blue InP quantum dot light-emitting diodes

Cite as: Appl. Phys. Lett. **120**, 091101 (2022); doi: 10.1063/5.0084416
Submitted: 6 January 2022 · Accepted: 14 February 2022 ·
Published Online: 28 February 2022

Guanding Mei,[1,2,3] Yangzhi Tan,[1,2,3] Jiayun Sun,[1,2,3] Dan Wu,[4] Tianqi Zhang,[1,3] Haochen Liu,[1,3] Pai Liu,[1,3] Xiao Wei Sun,[1,3,a)] Wallace C. H. Choy,[2,a)] and Kai Wang[1,3,a)]

AFFILIATIONS

[1]Guangdong University Key Lab for Advanced Quantum Dot Displays and Lighting, Shenzhen Key Laboratory for Advanced Quantum Dot Displays and Lighting, Department of Electrical and Electronic Engineering, Southern University of Science and Technology, Shenzhen 518055, China

[2]Department of Electrical and Electronic Engineering, The University of Hong Kong, Pokfulam Road, Hong Kong 999077, China

[3]Key Laboratory of Energy Conversion and Storage Technologies, Southern University of Science and Technology, Ministry of Education, Shenzhen 518055, China

[4]College of New Materials and New Energies, Shenzhen Technology University, Shenzhen 518118, China

[a)]**Authors to whom correspondence should be addressed:** sunxw@sustech.edu.cn; chchoy@eee.hku.hk; and wangk@sustech.edu.cn

ABSTRACT

Blue InP quantum dot light-emitting diodes (QLEDs) are promising candidates for environmental-friendly displays. To achieve efficient blue InP QLEDs through light extraction, the internal grating structure is a feasible way to extract waveguide modes, but it may bring complicated fabrication process and deteriorated electrical performance. In this work, we proposed an effective strategy to extract light from waveguide modes to air modes by using a thin hole transport layer (HTL), a high-index substrate, and substrate surface-roughening. Through optical tunneling, the thin HTL and the high-index substrate facilitate light transmission from waveguide modes to substrate modes. Thus, substrate surface-roughening can be applied to further extract light from enhanced substrate modes to air modes. As a result, light extraction efficiency has been significantly improved, leading to an external quantum efficiency enhancement from 2.1% to 2.8%, which is a record value among counterparts to date. This light extraction strategy is simple but effective to exploit the potential of high-efficiency (blue InP) QLEDs.

InP quantum dot light-emitting diodes (QLEDs) have been considered as strong environmentally benign candidates to fulfill the requirements of wide-color-gamut, low-cost, and versatility for next-generation display.[1–5] Until now, external quantum efficiencies (EQE) of 21.4% (Ref. 3) and 16.3% (Ref. 5) for red- and green-InP QLEDs have been achieved, respectively, which are comparable to their Cd-based counterparts.[6,7] However, although blue InP quantum dots (QDs) with photoluminescence quantum yield (PLQY) larger than 80% have been routinely obtained,[8,9] the highest reported EQE of blue InP QLEDs remained only 2.5% (Ref. 8), which is far from the figure of Cd-based blue QLEDs.[7] The light extraction efficiency (LEE) could be a key to breaking through the limited EQE of blue InP QLED. The EQE is determined by[10]

$$EQE = IQE \times LEE, \tag{1}$$

where IQE is internal quantum efficiency and LEE is defined by the ratio of the photons emitted to free space to all photons generated from the active region.[10] A crude LEE approximation[11–13] for planar structure QLED is given by

$$LEE = 1 - (1 - 1/n_{EML}^2)^{1/2}, \tag{2}$$

where n_{EML} is the refractive index of the emissive layer (EML). Equation (2) is based on ray-optics neglecting interference effects, showing how the larger EML index leads to smaller LEE as shown in Fig. 1(a). In the visible spectrum, our neat InP/ZnS QD film as an EML has a refractive index of ∼1.85. Therefore, the theoretical LEE of InP QLED is ∼15%, indicating that the remaining ∼85% of photons are trapped and dissipated in the device. This LEE is lower than that (20%) of conventional organic light-emitting diodes (OLEDs), whose EML indices are usually 1.6–1.7. With a higher index of EML, for

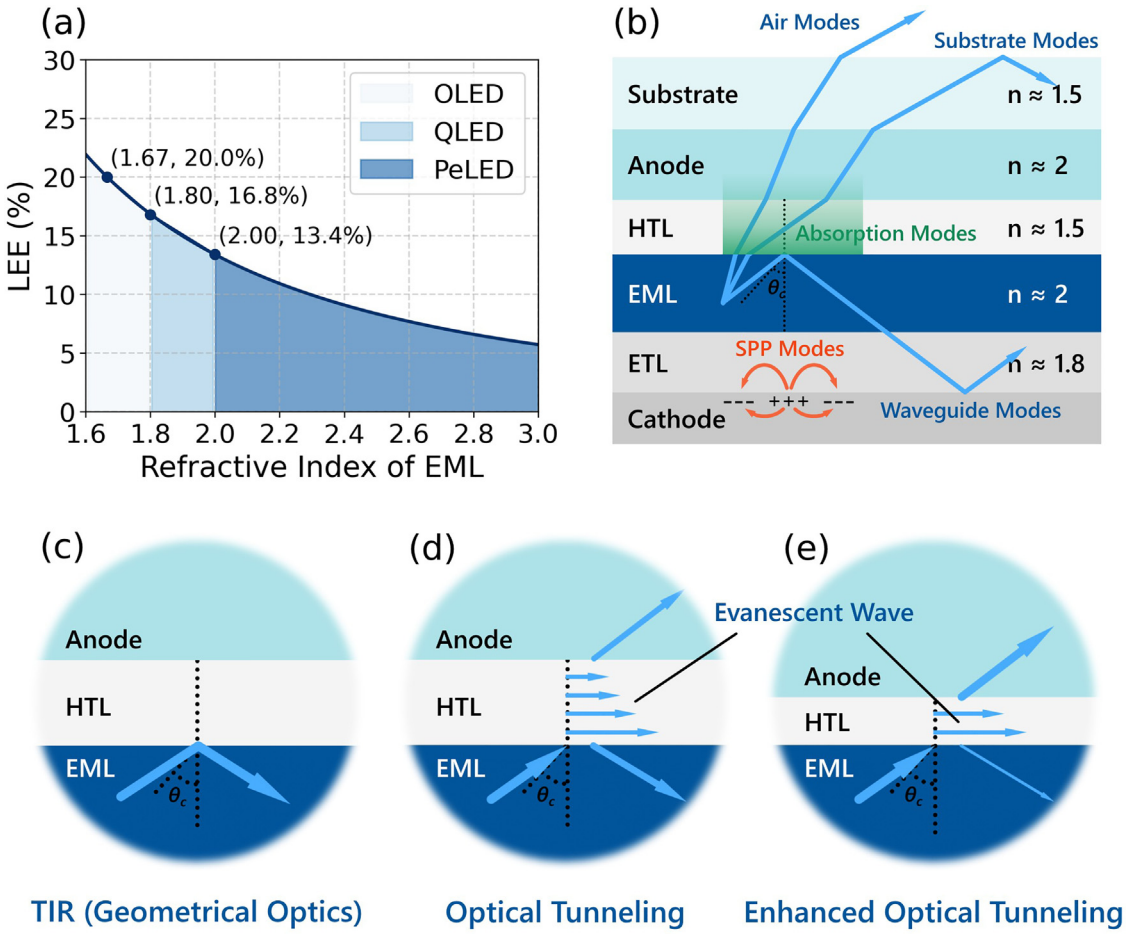

FIG. 1. Optical loss analysis in QLED. (a) LEE approximation as a function of the refractive index of EML for planar structure LEDs. (b) Schematic diagram of optical channels. (c) TIR at EML–HTL boundary based on geometrical optics. (d) FTIR or optical tunneling enables the propagation of light from EML to the anode. (e) Thinner HTL facilitates stronger optical tunneling.

example, the high-index perovskite in perovskite light-emitting diodes (PeLEDs), the limitation of LEE could be a severe problem.

The severe LEE limits destined us to analyze loss channels and develop suitable approaches to extract light. For the sake of simplification, five major optical channels are introduced in Fig. 1(b) (for the rigorous definition of optical channels, please refer to Refs. 14 and 15): (1) air modes, representing the light radiating into air; (2) substrate modes, representing the light trapped within the substrate by total internal reflection (TIR) at the interface between air and the substrate; (3) absorption modes, determining the absorption loss in the in-plane wavevector range overlapping with air modes and substrate modes; (4) waveguide modes, representing the light guided in functional layers including electrodes, the hole transport layer (HTL), the electron transport layer (ETL), and EML; (5) surface plasmon polariton (SPP) modes, corresponding to the evanescent wave. As reported in former studies,[15–17] in QLEDs, most of the light is trapped in substrate modes (∼20%) and waveguide modes (∼37%), only ∼15% of light emits to air. Significantly, QLEDs show stronger waveguide modes than OLED, which is primarily attributed to high indices of QDs.

According to the large waveguide modes in QLED, it tends to adopt the internal extraction structure (IES), which is constructed inside the device, to extract waveguide modes. Nevertheless, IES may exhibit disadvantages,[18] such as complicated fabrication process, deteriorated carrier injection, and large area limitation. Although an external extraction structure (EES) on the substrate-air interface could avoid these problems, the EES cannot extract waveguide modes, which traps many lights in QLEDs. In this work, we demonstrated that with the assistance of optical tunneling and high-index substrate, EES can be used to extract original waveguide modes.

According to Snell's law, Fig. 1(c) shows the incident light beyond the critical angle at EML–HTL interface should be totally reflected due to the index difference between HTL (n = ∼1.52) and EML (n = 1.8–2). This could be regarded as the main reason for waveguide modes on the premise of geometrical optics. However, from the perspective of wave optics, the light beyond the critical angle still has a chance to break through TIR. In typical QLEDs, the thickness of HTL is even thinner than the wavelength of the light, and the anode (ITO) has a relatively high refractive index of ∼2[11] [Fig. 1(d)]. In this case,

the light beyond the critical angle can partially penetrate the low-index HTL and arrive in the anode (ITO) because the evanescent waves can penetrate a distance in the normal direction then refracted into ITO. This phenomenon is called frustrated TIR (FTIR)[19] or optical tunneling. As shown in Fig. 1(e), derived from exponential attenuation of the evanescent wave field, the thin HTL facilitates stronger optical tunneling.

The blue InP QLED structure was glass/ITO (100 nm)/Poly(3,4-ethylenedioxythiophene)-poly(styrenesulfonate) (PEDOT:PSS) (30 nm)/MoO_3 (0.5 nm)/Poly[(9,9-dioctylfluorenyl-2,7-diyl)-co-(4,4′-(N-(4-sec-butylphenyl)diphenylamine)] (TFB) (30 nm)/QD (21 nm)/$Zn_xMg_{1-x}O$ nanoparticles (NPs, 50 nm)/Al (100 nm), as shown in Fig. 2. Notably, the MoO_3 layer was introduced to generate a pair of dipole-induced built-in electric fields that facilitate the hole injection and balance the carrier injection, where the detailed mechanism had been demonstrated in our previous work.[20,21] Because the thickness of MoO_3 is only 0.5 nm, we consider it as an interface modification of PEDOT:PSS instead of an individual layer. Optical tunneling allows the high-index substrate to convert waveguide modes into substrate modes. As shown in Figs. 2(a) and 2(b), once the light propagates to the anode–substrate interface through optical tunneling, a high-index substrate can sequentially transfer it to substrate modes. In this case, the EES aiming to extract substrate modes can also extract original waveguide modes [Fig. 2(c)].

Through numerical simulations, the effect of optical tunneling in our QLED devices is investigated, and the enhanced substrate modes by the high-index substrate are observed. As a result, our light extraction strategy leads to a 32% EQE enhancement from 2.14% to 2.82%. This is a feasible and low-cost light extraction approach to further improve the LEE and performance of QLEDs.

To theoretically analyze optical tunneling, the wavelength-dependent refractive indices of the QLED materials are needed. In Fig. 3(a), the indices of QD (∼1.83) and ZnMgO NPs (∼1.80) layers were measured by ellipsometry; the indices of ITO (∼1.95), PEDOT:PSS (∼1.52), and TFB (∼1.80) are provided by the commercial software Setfos. The normalized photoluminescence (PL) spectrum of InP QDs in solution is shown by the shaded region in Fig. 3(a), and we mainly focus on the refractive index in the wavelength region with strong PL. Because of the index difference between QD and PEDOT:PSS, when the incident angle is larger than the critical angle, evanescent waves were formed in PEDOT:PSS and decayed exponentially away from the interface. The penetration depth, at which the evanescent E-field drops to 1/e of its maximum value, can describe the attenuation of the evanescent wave field,

$$\delta = \frac{\lambda}{2\pi n_t \times \left[\left(\frac{n_i}{n_t}\right)^2 \sin^2\theta_i - 1\right]^{1/2}}, \tag{3}$$

where δ is the penetration depth, λ is the vacuum wavelength, θ_i is the incident angle, n_i is the refractive index of the incident medium, and n_t is the refractive index of transmitting medium. If $n_i = n_{EML}$, which is the index of EML, and $n_t = n_{HTL}$, which is the index of HTL, the penetration depth at the wavelength of 488 nm is shown in Fig. 3(b). It is found that the larger EML index produces smaller critical angle and faster field decay in large incident angle. In our structure, the index of TFB is close to the QD layer, we can simply ignore TFB to calculate the penetration depth with $n_{EML} = 1.83$ and $n_{HTL} = 1.52$ [red line in Fig. 3(b)]. In this case, the critical angle is 56°, and the minimum penetration depth is 76.2 nm. Therefore, the PEDOT:PSS thickness of 30 nm implies good optical tunneling through PEDOT:PSS.

The power dissipation spectrum of the blue InP QLED shown in Fig. 3(c) presents the power ratio radiated to each in-plane wavevector k_x, which is defined as

$$k_x = \frac{2\pi}{\lambda} n_i \sin\theta_i, \tag{4}$$

where n_i is the refractive index of ith layer, θ_i is the propagation angle in ith layer, and λ is the free space wavelength. We use the PL spectrum of InP QDs to perform the simulation; therefore, the power is mainly distributed in the blue spectral range. The dashed lines in Fig. 3(c) separate the regions of different optical modes. First, the substrate modes [Sub. region in Fig. 3(c)] trap a considerable part of the light. Because the light in the glass can be considered incoherent, the substrate modes are continuous; we suggest that the extraction structure should be randomly rough. Second, the waveguide modes [WG region in Fig. 3(c)] show the discrete distribution across the in-plane wavevector due to its interference properties; thus, the periodic nanostructures like grating are usually the solution to couple the waveguide mode.[22,23] However, if optical tunneling works as we predicted, the waveguide modes can be converted into the substrate modes by a high-index substrate. In this case, we can unify the extraction structure

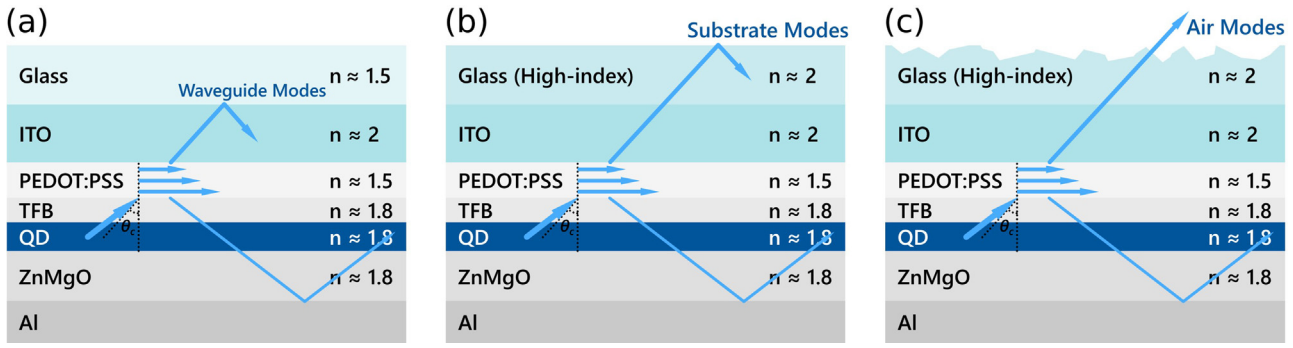

FIG. 2. Process of light extraction with optical tunneling. (a) Optical tunneling is enhanced by thin HTL, and the reflection is transferred to the anode-substrate interface. (b) High-index substrate converts waveguide modes to substrate modes. (c) Surface roughening converts substrate modes to air modes.

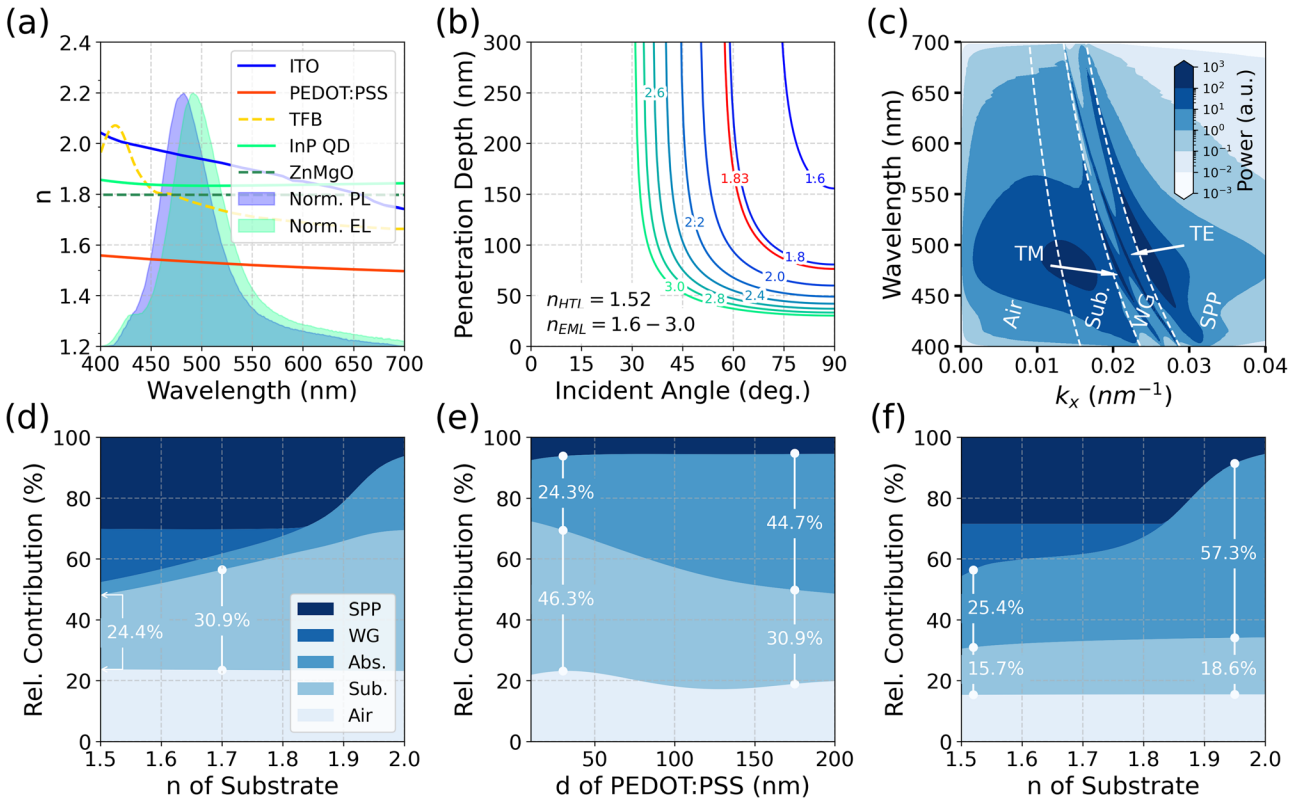

FIG. 3. (a) The refractive indices of the QLED materials in Fig. 2, the normalized PL spectrum of the InP QD, and the EL spectrum of the InP QLED. (b) Penetration depth of the evanescent wave vs angle of incidence for varied refractive index of EML at wavelength of 488 nm. (c) Power dissipation spectrum of the InP QLED; dashed lines separate the regions of different optical modes. Optical power distribution of different optical modes (d) vs refractive index of the substrate at PEDOT:PSS thickness of 30 nm, (e) vs PEDOT:PSS thickness at refractive index of the substrate of 2 and (f) vs refractive index of the substrate at PEDOT:PSS thickness of 600 nm.

into a random rough surface of the substrate, while the internal periodic nanostructures are bypassed. Meanwhile, the angular-dependent emission by the periodic structure can also be avoided. Third, the SPP region in Fig. 3(c) also shows a strong SPP. Because only transverse magnetic (TM) polarized waves can excite SPP,[24] Fig. 3(c) shows that SPP leads to a considerable dissipation of TM-polarized waves. In waveguide modes, we observed that compared to TE-polarized waves, TM-polarized waves have a smaller in-plane wavevector (i.e., smaller propagation angle). This means that the TM-polarized waves in the waveguide have priority to enter the high-index substrate through optical tunneling. However, the current QLED structure has dissipated too many TM-polarized waves in SPP modes. Thus, we predict that it would be a severe limitation for our light extraction approach.

The high-index substrate is the key to utilizing optical tunneling. The refractive index of substrate is swept from 1.5 to 2.0, and the simulated optical power distribution is shown in Fig. 3(d). The substrate modes continuously increase as the index of the substrate increases; meanwhile, the waveguide modes decrease. If we use glass with an index of 1.7 to replace common glass with an index of 1.5 as the substrate, the substrate modes can increase from 24.4% to 30.9%. The mode conversion is attributed to the reduced reflection at the ITO-substrate interface. In this process, the optical tunneling helps light penetrate the low-index HTL and reach the ITO-substrate interface, which is a prerequisite for the mode conversion. On the contrary, if optical tunneling does not exist, the high-index substrate would lose its ability to convert modes, because the critical angle of EML-PEDOT:PSS is close to that of EML-common glass due to the similar refractive index of PEDOT:PSS and the common glass. Thus, almost all the increase in substrate modes comes from optical tunneling.

To verify the existence of optical tunneling, the optical power distribution with different PEDOT:PSS thickness is investigated because the transmittance attenuation caused by thick intermediate medium is the main feature of optical tunneling. In Fig. 3(e), the substrate index is set to 2, which is close to the refractive index of ITO. In this case, most transmitted light through optical tunneling can be extracted to the substrate modes; then, we can evaluate the relationship between transmitted light and PEDOT:PSS thickness by substrate modes. If the PEDOT:PSS thickness increases from 30 to 175 nm, the substrate modes decrease from 46.3% to 30.9%, representing the transmittance attenuation. The light failed to penetrate the thick PEDOT:PSS is eventually absorbed in the stack; they are recognized as the increased absorption modes when the high-index substrate is applied. As we discussed in Fig. 3(b), the optical tunneling in our structure is not so sensitive to the thickness of PEDOT:PSS due to limited index difference between EML and HTL. Usually, the PEDOT:PSS thickness is adopted

TABLE I. Summary sheet of five groups of the QLED sample including their variables and EQE data.

Sample group	PEDOT: PSS thickness (nm)	n of Substrate	Substrate surface-roughening (Y/N)	Maximum EQE (%)	Average EQE (%)	Relative average EQE (%)
I (Control)	30	1.5	N	2.14	1.72	100
II	30	1.5	Y	2.07	1.86	108
III	30	1.7	N	1.99	1.66	97
IV	30	1.7	Y	2.42	1.98	115
V	10	1.7	Y	2.82	2.17	126

within 60 nm, although the thin PEDOT:PSS is preferred; there is no strict requirement for PEDOT:PSS to be very thin. However, if optical tunneling is blocked, the growth of the substrate modes is almost impossible. Assuming that PEDOT:PSS thickness is 600 nm, the optical power distribution vs substrate index is shown in Fig. 3(f). Even the waveguide modes disappeared, the increase in substrate modes is still hampered because the optical tunneling is almost blocked by the thick PEDOT:PSS. The increased absorption modes, whose in-plane wavevector range extends with the larger substrate index, contain more light that fails to tunnel through PEDOT:PSS. The limited substrate modes indicate the critical role of optical tunneling in our light extraction approach.

Five groups of QLEDs with different structures have been fabricated to verify the effectiveness of the aforesaid strategy. All QLEDs exhibited electroluminescence (EL) peak at 492 nm, which is 10 nm longer than that of PL [482 nm, see in Fig. 3(a)]. The variables among these groups are listed in Table I, where the data of maximum EQE, average EQE, and relative average EQE (compared with control sample group I) for each group are also available. It is

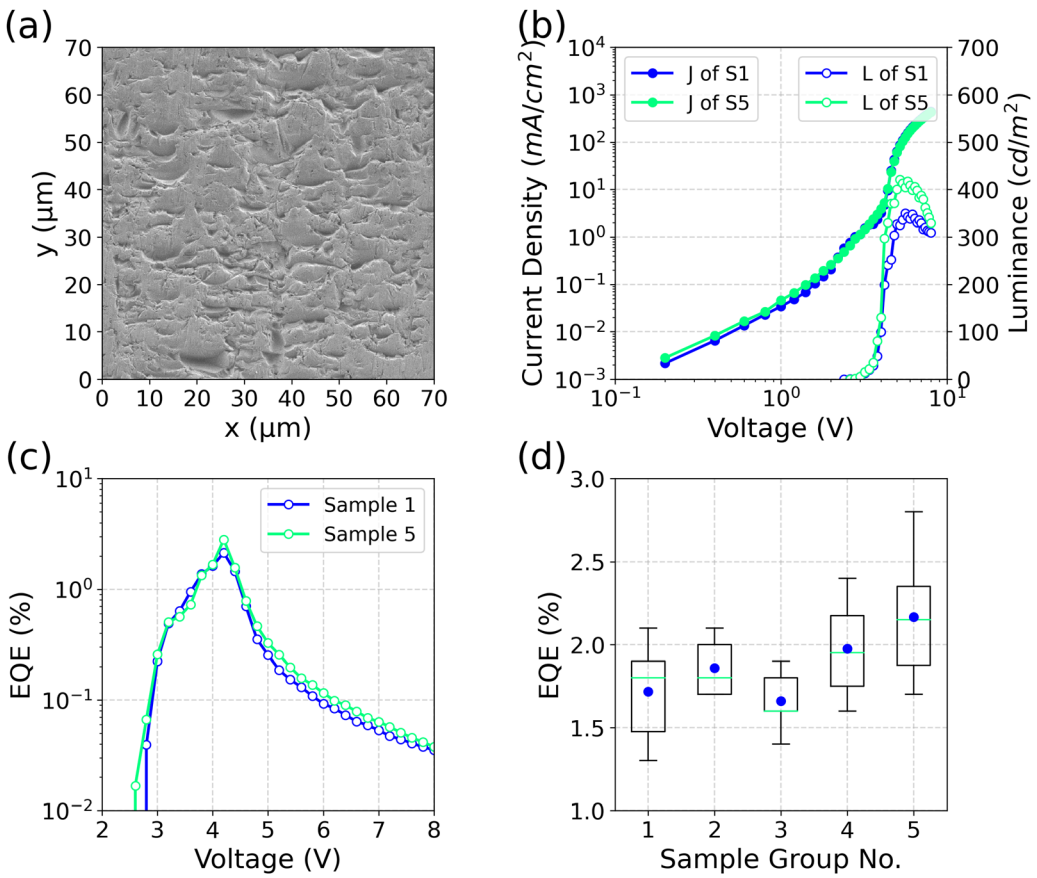

FIG. 4. (a) The surface morphology of the surface-roughened substrate, characterized by SEM. (b) J–V–L characteristics and (c) EQE–J characteristics of the QLEDs samples of group I and V. (d) Statistics of EQE of five groups, five to six samples for each group.

worth mentioning that only photons emitted from the substrate surface of QLEDs have been collected for the measurement of luminance and EQE, and only in this case, we can accurately evaluate the QLEDs performance with light extraction structures.

The substrate of samples in group II, IV, and V has been treated with acid-etching and then with sandpaper sanding to generate a roughened substrate surface [Fig. 4(a)], and this roughened surface can extract light from substrate modes to air modes by inhibiting the TIR in the interface of substrate/air. These QLEDs with the surface-roughened substrate (group II) exhibited 8% higher EQE on average compared with that with the planar 1.5-index substrate (group I).

However, if only replace the 1.5-index substrate by the 1.7-index one, the LEE (air modes) remained nearly the same according to the simulation result in Fig. 3(d). Although the substrate modes have been improved through enhanced optical tunneling by a 1.7-index substrate, the air modes remain almost unchanged without any extra light extraction structure. As a result, the average EQE in group III (1.66%) is close to that of the group I (1.72%), which fits well with the simulation result. Furthermore, when combing the 1.7-index substrate with substrate surface-roughening, the enhanced substrate modes could be effectively extracted to the air modes, leading to a higher LEE and EQE. Comparing the average EQE of group I (1.72%) and IV (1.98%), the improvement is ∼15%. Because the treatments of QLEDs of group I to IV do not include internal modification inside the device, the electrical property of the device is unchanged. In addition, the 1.7-index glass does not change the SPP modes in Fig. 3(a), and the fluorescent lifetime of QDs is hardly affected. According to Fig. 3(d), LEE ≈24% for sample group I, we can derive the IQE ≈9% from IQE = EQE/LEE. In summary, IQE should keep constant in our strategy, the EQE improvement from group I to IV is primarily attributed to the LEE enhancement. What is more, the thinner PEDOT:PSS also benefits the performance of blue InP QLEDs. The average EQE of group V (2.17%) improved by 10% compared with group IV (1.98%). The improvement could be attributed to the enhanced optical tunneling through PEDOT:PSS and effectively extracted substrate modes. Nevertheless, according to the simulation result [see in Fig. 3(e)], the optical improvement should not be so large as 10%, and we suppose that there should be an extra positive effect of thinner PEDOT:PSS, e.g., improved hole mobility and more matched energy level alignment.[25]

As a result, the maximum EQE of group V comes to 2.82%, which is 32% higher than that of the control sample (2.14% of group I) as shown in Fig. 4(c). The maximum luminance also increased from 350 to 421 cd/m^2 [see in Fig. 4(b)]. The statistics of EQE of the five groups is also given in Fig. 4(d), showing that the strategy used in this work has good repeatability.

In conclusion, through optical tunneling, the high-index substrate can convert waveguide modes to substrate modes. Following the surface roughening, the trapped light is extracted from the substrate to air. Based on our light extraction strategy, the maximum efficiency improvement of 32% is obtained in blue InP QLED. Moreover, the waveguide modes can be extracted without introducing any internal extraction structure, thereby avoiding high cost and electrical damage. Through theoretical analysis and experimental verification, we believe that this comprehensive light extraction strategy is expected to boost the efficiency of blue InP QLEDs as well as other types of QLEDs.

This work was supported by the National Key Research and Development Program (Nos. 2017YFE0120400 and 2019YFB1704600), National Natural Science Foundation of China (Nos. 61875082, 61905107, and 62005115), Key-Area Research and Development Program of Guangdong Province (No. 2019B010924001), and Guangdong University Key Laboratory for Advanced Quantum Dot Displays and Lighting (No. 2017KSYS007), Shenzhen Peacock Team Project (No. KQTD2016030111203005), the General Research Fund (Grant Nos. 17200518, 17201819, and 17211220) and Collaboration Research Fund (No. C7035-20G) from Hong Kong Special Administrative Region, China.

AUTHOR DECLARATIONS

Conflict of Interest

The authors have no conflicts to disclose.

Author Contributions

G.M. and Y.T. contributed equally to this work.

DATA AVAILABILITY

The data that support the findings of this study are available from the corresponding authors upon reasonable request.

REFERENCES

[1]F. P. García de Arquer, D. V. Talapin, V. I. Klimov, Y. Arakawa, M. Bayer, and E. H. Sargent, Science **373**, eaaz8541 (2021).
[2]W. Zhang, S. Ding, W. Zhuang, D. Wu, P. Liu, X. Qu, H. Liu, H. Yang, Z. Wu, K. Wang, and X. W. Sun, Adv. Funct. Mater. **30**, 2005303 (2020).
[3]Y. H. Won, O. Cho, T. Kim, D. Y. Chung, T. Kim, H. Chung, H. Jang, J. Lee, D. Kim, and E. Jang, Nature **575**, 634 (2019).
[4]Z. Wu, P. Liu, W. Zhang, K. Wang, and X. W. Sun, ACS Energy Lett. **5**, 1095 (2020).
[5]W.-C. Chao, T.-H. Chiang, Y.-C. Liu, Z.-X. Huang, C.-C. Liao, C.-H. Chu, C.-H. Wang, H.-W. Tseng, W.-Y. Hung, and P.-T. Chou, Commun. Mater. **2**, 96 (2021).
[6]D. Chen, D. Chen, X. Dai, Z. Zhang, J. Lin, Y. Deng, Y. Hao, C. Zhang, H. Zhu, F. Gao, and Y. Jin, Adv. Mater. **32**, 2006178 (2020).
[7]H. Shen, Q. Gao, Y. Zhang, Y. Lin, Q. Lin, Z. Li, L. Chen, Z. Zeng, X. Li, Y. Jia, S. Wang, Z. Du, L. S. Li, and Z. Zhang, Nat. Photonics **13**, 192 (2019).
[8]K. H. Kim, J. H. Jo, D. Y. Jo, C. Y. Han, S. Y. Yoon, Y. Kim, Y. H. Kim, Y. H. Ko, S. W. Kim, C. Lee, and H. Yang, Chem. Mater. **32**, 3537 (2020).
[9]H. Zhang, X. Ma, Q. Lin, Z. Zeng, H. Wang, L. S. Li, H. Shen, Y. Jia, and Z. Du, J. Phys. Chem. Lett. **11**, 960 (2020).
[10]J.-I. Shim and D.-S. Shin, Nanophotonics **7**, 1601 (2018).
[11]G. Mei, D. Wu, S. Ding, W. C. H. Choy, K. Wang, and X. W. Sun, IEEE Photonics J. **12**, 7902605 (2020).
[12]N. C. Greenham, R. H. Friend, and D. D. C. Bradley, Adv. Mater. **6**, 491 (1994).
[13]T. Tsutsui, M. Yahiro, H. Yokogawa, K. Kawano, and M. Yokoyama, Adv. Mater. **13**, 1149 (2001).
[14]A. Buckley, *Organic Light-Emitting Diodes (OLEDs): Materials, Devices and Applications* (Elsevier, 2013).
[15]G. Tan, R. Zhu, Y. S. Tsai, K. C. Lee, Z. Luo, Y. Z. Lee, and S. T. Wu, J. Phys. D **49**, 315101 (2016).
[16]H. Liang, Z. Luo, R. Zhu, Y. Dong, J. H. Lee, J. Zhou, and S. T. Wu, J. Phys. D **49**, 145103 (2016).
[17]H. Liang, R. Zhu, Y. Dong, S.-T. Wu, J. Li, J. Wang, and J. Zhou, Opt. Express **23**, 12910 (2015).
[18]Y. Jiang, S. Chen, G. Li, H. Li, and H. S. Kwok, Adv. Opt. Mater. **2**, 418 (2014).
[19]S. Zhu, A. W. Yu, D. Hawley, and R. Roy, Am. J. Phys. **54**, 601 (1986).
[20]X. Xiao, K. Wang, T. Ye, R. Cai, Z. Ren, D. Wu, X. Qu, J. Sun, S. Ding, X. W. Sun, and W. C. H. Choy, Commun. Mater. **1**, 81 (2020).

[21]Y. Tan, W. Zhang, X. Xiao, J. Sun, J. Ma, T. Zhang, G. Mei, Z. Wang, F. Zhao, D. Wu, W. C. H. Choy, X. W. Sun, and K. Wang, Appl. Phys. Lett. **119**, 221105 (2021).
[22]S. Wang, X. Dou, L. Chen, Y. Fang, A. Wang, H. Shen, and Z. Du, Nanoscale **10**, 11651 (2018).
[23]T.-B. Lim, K. H. Cho, Y.-H. Kim, and Y.-C. Jeong, Opt. Express **24**, 17950 (2016).
[24]A. R. Zakharian, Jv. Moloney, and M. Mansuripur, Opt. Express **15**, 183 (2007).
[25]J. Lu, W. Feng, G. Mei, J. Sun, C. Yan, D. Zhang, K. Lin, D. Wu, K. Wang, and Z. Wei, Adv. Sci. **7**, 2000689 (2020).